

## Quantifying oxygen diffusion in ZnO nanobelt

Jin Liu, Puxian Gao, Wenjie Mai, Changshi Lao, and Zhong L. Wang<sup>a)</sup>  
*School of Materials Science and Engineering, Georgia Institute of Technology, Atlanta, Georgia 30332*

Rao Tummala  
*School of Electrical and Computer Engineering, Georgia Institute of Technology, Atlanta, Georgia 30332*

(Received 28 January 2006; accepted 5 June 2006; published online 11 August 2006)

A method is presented for quantifying oxygen diffusion behavior in a nanodevice fabricated using individual ZnO nanowire/nanobelt. A nanodevice was built using a single nanobelt. Defects are introduced into nanobelt during specific nanofabrication procedure. Then, after the device being exposed to atmosphere for several days, oxygen in air diffused into the nanobelt and significantly changed the conductivity of the device. By comprising the experimentally measured conductivity and that of simulated result, the diffusion coefficient of oxygen in ZnO nanowires/nanobelts has been derived. © 2006 American Institute of Physics. [DOI: 10.1063/1.2236214]

Carbon nanotubes (CNTs),<sup>1</sup> silicon nanowires,<sup>2</sup> and ZnO nanowires/nanobelts are the most outstanding examples of one dimensional (1D) nanostructures that have been extensively studied. It is known that the conductivity of these 1D nanostructures is strongly affected by doping, such as CNT can be doped with nitrogen, Si can be doped with boron, and ZnO can be doped with Mg. In comparison to both carbon and silicon, the conductivity of ZnO can be tuned by changing the oxygen deficiency or vacancies. Controlling oxygen diffusion and distribution in ZnO is important for understanding its electronic and optical properties.

ZnO is an important material as resonators for microelectromechanical systems,<sup>3</sup> optical material for fabricating blue light emitting diodes (LEDs),<sup>4</sup> and piezoelectric and semiconducting materials for actuators. Field effect transistor,<sup>5</sup> gas sensor,<sup>6</sup> and pH meter<sup>7</sup> using ZnO nanowire/nanobelts have been reported, the performance of which strongly relies on the oxygen deficiency and distribution in ZnO nanostructures. In this letter, we report our study on the diffusion of oxygen in nanodevices built using a single ZnO nanobelt. The diffusion coefficient of oxygen in ZnO nanobelt has been derived by comparing the measured data with the simulation based on finite element analysis (FEA) model. This study will be helpful for predicting the stability of the devices made using ZnO nanowire/nanobelt.

ZnO nanobelts are synthesized through a high temperature solid-vapor process, as reported elsewhere.<sup>8</sup> The synthesized ZnO nanobelts have a size of around 200 nm and length of up to 5  $\mu\text{m}$ . According to Pan *et al.*,<sup>9</sup> ZnO nanowire/nanobelt is wurtzite (hexagonal) structure and grows along either [0001]/[01 $\bar{1}$ 0] direction. The synthesized ZnO nanobelts are transferred from the Al<sub>2</sub>O<sub>3</sub> substrate to prepatterned Au electrodes via either dielectrophoresis<sup>10</sup> or micromanipulation method. The prepatterned Au electrodes are fabricated on 100 nm Si<sub>3</sub>N<sub>4</sub> that is deposited on Si wafer using plasma enhanced chemical vapor deposition (PECVD) through a typical lift-off process. SiH<sub>4</sub> and NH<sub>3</sub>, which acted as precursors for the reaction, are plasmonized at 30 kV and 300 °C. As a result, Si<sub>3</sub>N<sub>4</sub> is deposited on the surface of Si at a rate of 50 Å/min. Then, AZ5214-E photoresist is spun on

and exposed under UV light using MJB-3 mask aligner. After developing, Ti/Au with a thickness of 20/200 nm are deposited through e-beam evaporation to form the Au electrodes. To reduce the contact resistance, focused ion beam (FIB) microscopy is employed to deposit Pt on the contacts between ZnO and Au electrodes. The deposited Pt is not pure metal because it is formed from the dissociation of organic Pt precursor as a result of Ga<sup>+</sup> bombardment. Current-voltage measurements indicate that the Pt deposited contact between ZnO and Au was Ohmic contact. The ZnO nanobelt placed between Au electrodes is subsequently deposited with 50 nm Si<sub>3</sub>N<sub>4</sub> by PECVD for the purpose of isolating ZnO nanobelt from contacting the atmosphere. Also, PECVD procedure introduces defects to ZnO nanobelt, and the defects are also isolated in ZnO nanobelt by the Si<sub>3</sub>N<sub>4</sub> layer.

In order to investigate the diffusion of oxygen into the ZnO nanobelt, half of the deposited Si<sub>3</sub>N<sub>4</sub> is milled off by FIB. The current and voltage (10 kV, 1 pA) of the milling parameters are chosen to be very small to make sure that the milling process does not introduce extra damage or defects in the nanobelt. The resultant schematic structure of the device is shown in Fig. 1(a). Two samples of ZnO nanobelts with different lengths and diameters are prepared through the above procedures. The two samples may also be slightly different in concentration of defects as introduced by the fabrication process.

The current-voltage characteristic of the ZnO nanobelt is then measured by an HP 4156A precision semiconductor analyzer immediately after the ion milling. Additional measurement is done on a daily basis throughout one week. For an easy comparison, conductivity is used to represent the electronic property of the nanobelt. The conductivity change of ZnO nanobelt over time could be expressed as

$$\Delta\sigma(t) = \Delta G(t) \cdot \frac{l}{A}, \quad (1)$$

where  $\Delta G(t)$  is conductance change over time,  $l$  is the length of the nanobelt, and  $A$  is its cross section. The measured conductivity change as a function of time is shown in Fig. 1(b).

It is well known that the conductivity of ZnO comes from the oxygen vacancies. With considering the large surface area of the nanowire/nanobelt, surface conductivity also

<sup>a)</sup> Author to whom correspondence should be addressed; electronic mail: zhong.wang@mse.gatech.edu

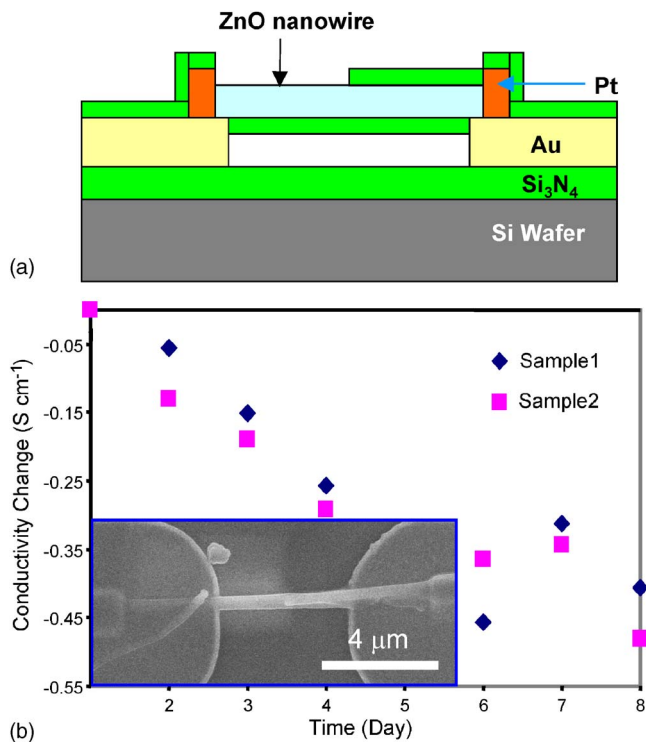


FIG. 1. (Color online) (a) Schematic of ZnO nanowire placed on prepatterned Au electrodes after Si<sub>3</sub>N<sub>4</sub> deposition. (b) Conductivity change of ZnO nanowires over time. The inset shows the scanning electron microscopy (SEM) image of the fabricated device.

contributes to the final resultant data. If the surface adsorption occurs quickly after the device was fabricated, the change in conductance is mainly contributed by the change in oxygen vacancy concentration in the volume. As more oxygen diffuses through the surface to fill in the oxygen vacancies, the conductivity of the nanowire/nanobelt is expected to drop. A quantitative understanding of this process may derive the diffusion coefficient of oxygen in ZnO nanostructures.

In order to explain the behavior of the observed conductivity change, we have carried out a simulation based on the following assumptions. First of all, the defects are assumed to be uniformly distributed in the volume of the nanobelt at the beginning since nanobelt's cross section is relatively small. Secondly, the oxygen molecules in the atmosphere adhere to the surface of ZnO and break down to single oxygen atoms, which has the same molecular concentration as the oxygen molecule in the atmosphere (22% in volume). This is concluded from the fact that oxygen molecules adsorbed on the surface of the ZnO nanobelts are decomposed into single oxygen atoms with the presence of oxygen vacancies. The oxygen vacancies on the surface are intrinsic as well as created by plasma effect during the PECVD process. The presence of a large number of oxygen vacancies together with the constant diffusion of oxygen atoms into the bulk of the ZnO nanobelts drives the decomposition of the molecules. Therefore, it is assumed that the concentration of the single oxygen atoms on the surface of the ZnO nanobelts is constant and the same as that of oxygen molecules in the atmosphere. This is to set the boundary condition. Lastly, Si<sub>3</sub>N<sub>4</sub> acts as an O<sub>2</sub> insulator between atmosphere and ZnO; thus, there is no oxygen penetration into the nanobelt at the portion covered by Si<sub>3</sub>N<sub>4</sub> film and oxygen could only diffuse

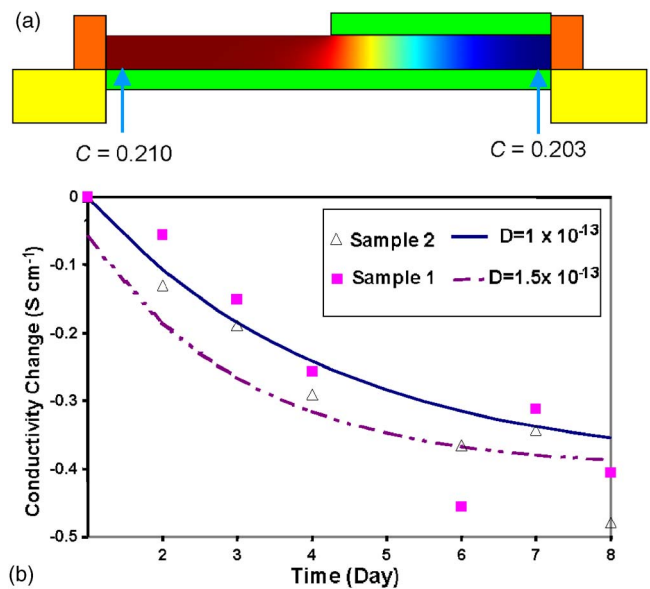


FIG. 2. (Color online) (a) Simulated oxygen distribution on the eighth day after ion milling process. (b) Illustration of curve fitting to determine the oxygen diffusion coefficient. The continuous lines represent the simulated results while the dots represent the experimental results. The geometrical parameters are extracted from the SEM images of the tested nanowires. The electron mobility is 17 cm<sup>2</sup>/V s, which is from literature (Ref. 11).

through the exposed region to the nanobelt. Based on these assumptions, a FEA model is established using COMSOL Multiphysics. Simulation is carried out starting from Fick's law. Figure 2(a) illustrates the oxygen concentration distribution profile on the eighth day.

As an *n*-type semiconductor, it is known that the conductivity in ZnO could be expressed as

$$\sigma(t) \approx e \cdot n(t) \cdot \mu^e, \quad (2)$$

where  $\sigma(t)$  is the conductivity of ZnO as a function of time,  $e$  is the charge of an electron,  $n(t)$  is total electron concentration in the volume as a function of time, and  $\mu^e$  is the electron mobility in ZnO.  $n(t)$  could be expressed as the difference between the initial total oxygen vacancies ( $V_D$ )

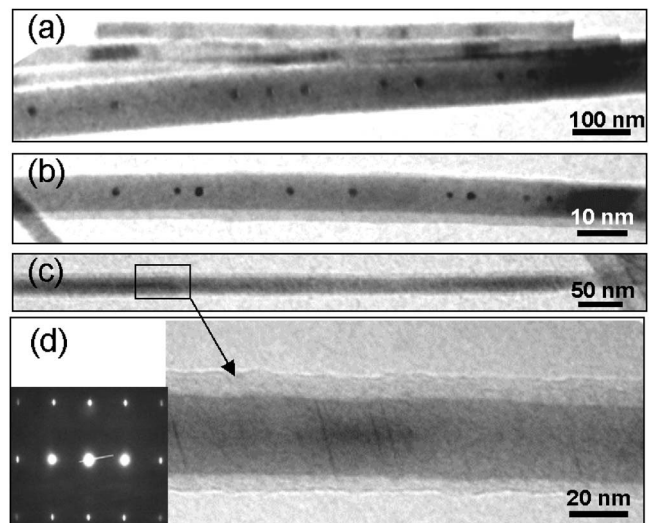


FIG. 3. TEM images of ZnO [(a) and (b)] nanobelts and (c) nanowire after Si<sub>3</sub>N<sub>4</sub> deposition, showing the defects introduced in the volume as a result of nanofabrication.

and the vacancies that are filled by oxygen diffused through the surface,

$$n(t) = \frac{2 \left( V_D - \int_0^d \int_0^l C(x,y,t) \cdot dx dy \right)}{V}, \quad (3)$$

where  $V_D$  is the total oxygen vacancies,  $d$  is the diameter of the ZnO nanobelt or the thickness of the nanobelt (please

note that the nanobelt is half protected by the nitride layer),  $l$  is the length of ZnO nanobelt, and  $C(x,y,t)$  is the concentration of oxygen atoms diffused through the surface and distributed at a particular point  $(x,y)$  from the surface at time  $t$ . Each oxygen vacancy contributes two free electrons.  $V$  is the volume of ZnO nanobelt.

At two different time intervals,  $t_1$  and  $t_2$ ,

$$\Delta n(t) = n(t_2) - n(t_1) = \frac{2 \left( \int_0^d \int_0^l C(x,y,t_1) \cdot dx dy - \int_0^d \int_0^l C(x,y,t_2) \cdot dx dy \right)}{V}. \quad (4)$$

Therefore, combining Eqs. (2) and (4), we get

$$\frac{\Delta \sigma(t)}{e \cdot \mu^e} = -2 \Delta C_o(t), \quad (5)$$

where  $\Delta C_o(t)$  is the concentration change of oxygen vacancies due to diffusion.  $\Delta C_o(t)$  could be obtained from simulation, and  $\mu^e$  is known for ZnO nanowire/nanobelt through a previous measurement to be around  $17 \text{ cm}^2/\text{V s}$ .<sup>11</sup> So it is possible to plot a curve of conductivity versus time change as shown in Fig. 2(b), which could derive the oxygen diffusion coefficient by fitting the simulated curve with the measured data.

Oxygen diffusion coefficient is used to represent the actual diffusion process in the material. For ZnO, there has been a report that the mechanism of oxygen diffusion is interstitial and the coefficient is in the order of  $10^{-15} - 10^{-17} \text{ cm}^2/\text{s}$ , depending on the growth temperature.<sup>12</sup> It is important to obtain the diffusion coefficient of ZnO nanostructures, which could be very useful for sensor applications. Using the simulated data, it is clear that the two sets of data fit between  $1 \times 10^{-13}$  and  $1.5 \times 10^{-13} \text{ cm}^2/\text{s}$ . The two samples are apparently different in geometry and may be different in defect concentration. The measured data for the two samples show slightly different trends although the data points are within the range. In any case, the result is two to four orders of magnitude larger than that of pure bulk ZnO.

To explain the large oxygen diffusion coefficient in the nanobelt, the structure of the ZnO nanobelts of the same batch has been examined by transmission electron microscope (TEM) post- $\text{Si}_3\text{N}_4$  deposition, as shown in Fig. 3. From the images, it is apparent that there are point and planar defects being introduced during the  $\text{Si}_3\text{N}_4$  formation process. These defects dramatically enhance the oxygen diffusion process and the effect is presented in the measured oxygen diffusion coefficient.

In summary, a method for quantifying oxygen diffusion behavior in a nanodevice fabricated using individual ZnO nanowire/nanobelt is presented. A nanodevice was built using a single nanobelt, but due to the procedures introduced in nanofabrication, defects are introduced in the nanobelt, resulting in an enhanced electrical conductivity due to the presence of oxygen vacancies. Then, after the device being exposed to atmosphere for several days, oxygen in air diffused into the nanobelt and significantly changed the conductivity of the device. By comprising the experimentally measured conductivity and that simulated using finite element analysis (FEA), we were able to derive the diffusion coefficient of oxygen in ZnO nanowires/nanobelts.

Thanks for the support from NSF, the NASA Vehicle Systems Program and Department of Defense Research and Engineering (DDR&E), and the Defense Advanced Research Projects Agency (Award No. N66001-04-1-8903). The authors would like to thank Jinhui Song for stimulating discussions.

<sup>1</sup>S. Iijima, *Nature (London)* **354**, 56 (1991).

<sup>2</sup>J. Hu, O. Min, P. Yang, and C. M. Lieber, *Nature (London)* **399**, 48 (1999).

<sup>3</sup>M. Hoffmann, T. Leuerer, R. Liedtke, U. Bottger, W. Mokwa, and R. Waser, *Integr. Ferroelectr.* **50**, 21 (2002).

<sup>4</sup>D.-K. Hwang, S.-H. Kang, J.-H. Lim, E.-J. Yang, J.-Y. Oh, J.-H. Yang, and S.-J. Park, *Appl. Phys. Lett.* **86**, 222101 (2005).

<sup>5</sup>M. S. Arnold, P. Avouris, Z. W. Pan, and Z. L. Wang, *J. Phys. Chem. B* **107**, 659 (2003).

<sup>6</sup>H. T. Wang, B. S. Kang, F. Ren, L. C. Tien, P. W. Sadik, D. P. Norton, S. J. Pearton, and J. Lin, *Appl. Phys. Lett.* **86**, 243503 (2005).

<sup>7</sup>B. S. Kang, F. Ren, Y. W. Heo, L. C. Tien, D. P. Norton, and S. J. Pearton, *Appl. Phys. Lett.* **86**, 112105 (2005).

<sup>8</sup>Z. L. Wang, *J. Phys.: Condens. Matter* **16**, R829 (2004).

<sup>9</sup>Z. W. Pan, Z. R. Dai, and Z. L. Wang, *Science* **291**, 1947 (2001).

<sup>10</sup>J. Liu, C. Lao, R. R. Tummala, and Z. L. Wang, *ICEPT2005, 1-4 2005* (IEEE CMPT, Shenzhen, China, August 2005).

<sup>11</sup>F. Zhiyong, W. Dawei, C. Pai-Chun, T. Wei-Yu, and J. G. Lu, *Appl. Phys. Lett.* **85**, 5923 (2004).

<sup>12</sup>A. Sabioni, W. Ferraz, and F. Millot, *J. Nucl. Mater.* **278**, 364 (2000).